

A New Method To Determine the Generation of Hydroxyl Radicals in Illuminated TiO₂ Suspensions

Peter F. Schwarz and Nicholas J. Turro*

Department of Chemistry, Columbia University, New York, New York 10027

Stefan H. Bossmann and Andre M. Braun

Lehrstuhl für Umweltmesstechnik am Engler-Bunte-Institut der Universität Karlsruhe, 76128 Karlsruhe, Germany

Aboel-Magd A. Abdel Wahab

Faculty of Science, Assiut University, Assiut, A. R. E. Egypt 71516

Heinz Dürr

Fb.:11.2 Organische Chemie, Universität des Saarlandes, 66123 Saarbrücken, Germany

Received: April 16, 1997; In Final Form: June 24, 1997[⊗]

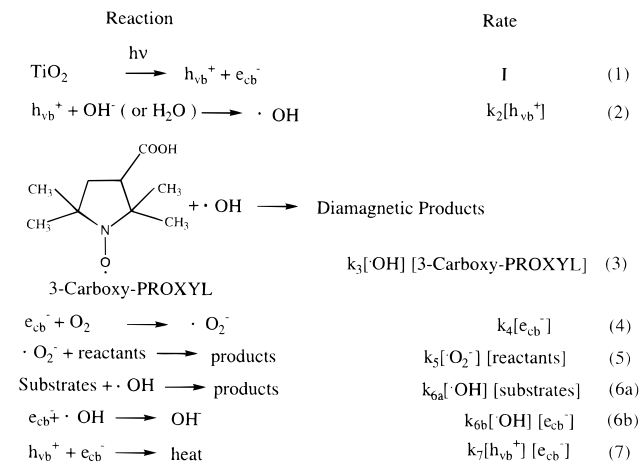
The generation of hydroxyl ($\cdot\text{OH}$) radicals produced by irradiation of aqueous TiO₂ suspensions was investigated by electron paramagnetic resonance (EPR) and product analysis employing a stable free nitroxide radical (3-carboxyproxyl) as a spin trap of $\cdot\text{OH}$. Product analysis demonstrated that the attack of $\cdot\text{OH}$ on 3-carboxyproxyl produces a diamagnetic product (proxyl–NH) with a trapping efficiency of ca. 80%. It could also be shown that a small amount of the nitroxides is reduced by conduction band electrons. The rate of formation of $\cdot\text{OH}$ could be determined by monitoring the time dependence of the decrease in the concentration of 3-carboxyproxyl monitored by EPR spectroscopy or the time dependence of the increase in the concentration of proxyl–NH monitored by gas chromatography analysis. The rate of formation of $\cdot\text{OH}$ serves as a mechanistic parameter to investigate the mechanism of formation of this reactive species by the photoexcitation of TiO₂. The dependence of the rate of formation of $\cdot\text{OH}$ was shown to be a linear function of light intensity at low intensities. It was observed that molecular oxygen, a good scavenger of conduction band electrons, only slightly influences the rate of formation of $\cdot\text{OH}$ and supports the production of $\cdot\text{OH}$ from photogenerated holes. Addition of selected anions to the photolysis mixtures results in a diminished rate of disappearance of the spin trap as the result of a competition between the spin trap and the anion for $\cdot\text{OH}$. From a Stern–Volmer analysis of the data, the rate constant for the reaction of hydroxyl radicals with the anions was determined.

Introduction

During the past two decades following the discoveries of Fujishima and Honda,^{1,2} considerable research has been devoted to the investigation of the mechanism of the photoelectrochemistry of semiconductors such as TiO₂, especially for air-saturated aqueous solutions of organic molecules. This research has been motivated in part because of the potential for the use of irradiation of semiconductors as catalysts and as a means of mineralization and purification of organic pollutants in environmental aqueous media.^{3–6}

From this research a useful working paradigm has evolved (Scheme 1) which views the mineralization of organic pollutants as originating from an initial process in which the absorption of a photon, possessing an energy that is greater than that of the band gap of the semiconductor particle, causes the promotion of an electron from the valence band (vb) of the semiconductor to the conduction band (cb) of the semiconductor. This process generates a positive “hole”, h_{vb}^+ , at the valence band edge of the semiconductor particle and an electron, e_{cb}^- , in the conduction band of the particle (eq 1). A number of processes can follow to initiate the mineralization of organic materials present in the irradiated suspension containing the semiconductor, e.g.,

SCHEME 1



(1) h_{vb}^+ and e_{cb}^- can react directly with organic species adsorbed on the surface of the particle, (2) h_{vb}^+ and e_{cb}^- can be transformed into high-energy chemical species which react with the adsorbed organic species, or (3) h_{vb}^+ and e_{cb}^- can be transformed into high energy chemical species which can diffuse into the aqueous phase and then react with dissolved organic

[⊗] Abstract published in *Advance ACS Abstracts*, August 15, 1997.

species. In the case of TiO_2 it is commonly accepted that h_{vb}^+ is transformed into hydroxyl radicals ($\cdot\text{OH}$, eq 2) and that in the presence of dissolved molecular oxygen e^- is converted into the superoxide anion ($\cdot\text{O}_2^-$, eq 4). The quantum efficiency of the production of reactive species depends on the efficiency of eq 1 and the efficiency by which the reactive species produced in eqs 2 and 4 can initiate mineralization. It is generally accepted that hole/electron annihilation (eq 7) to produce unproductive heat is a very fast process² (occurring on the nanosecond time scale) that determines the efficiency of mineralization, especially under conditions for which the organic material is not strongly adsorbed on the surface of the particle (see Scheme 1).

It is generally assumed that the $\cdot\text{OH}$ radicals produced in eq 2 are the major species responsible for the mineralization of organic pollutants.^{7,8} This premise is rendered plausible because of the lower reducing potential of a conduction band electron compared to the oxidizing power of a valence band hole and because most reducible substrates may not compete kinetically with molecular oxygen in trapping photogenerated conduction band electrons. Convincing evidence for the generation of $\cdot\text{OH}$ upon irradiation of aqueous solutions of TiO_2 has been obtained from the use of spin traps^{9–13} capable of scavenging the $\cdot\text{OH}$ radicals and producing a characteristic nitroxide which can be detected by electron paramagnetic resonance (EPR). Jaeger and Bard⁹ first demonstrated that $\cdot\text{OH}$ could be scavenged by spin traps such as 5,5-dimethyl-1-pyrroline *N*-oxide (DMPO), for which a $\cdot\text{OH}$ -trapping efficiency (chemical yield of $\cdot\text{OH}$ adduct based on DMPO) of ca. 33% has been estimated.¹³ In addition to serving as a means of demonstrating the formation of $\cdot\text{OH}$, the spin-trapping technique has been usefully employed to investigate the mechanism of the processes implied in eqs 1–7, including the absolute quantum efficiency of the formation of $\cdot\text{OH}$.

In the present report we evaluate the technique employing an EPR active nitroxide, 3-carboxyproxyl, as the spin trap for which reaction with $\cdot\text{OH}$ produces diamagnetic EPR inactive products. The premise behind the selection of the method is the validity of the paradigm described above for the role of $\cdot\text{OH}$ as the dominant oxidizing species produced upon irradiation of aqueous solutions of TiO_2 and the expectation that the radical–radical coupling reaction between a nitroxide and $\cdot\text{OH}$ would be extremely rapid (eq 3). Under these assumptions, the time dependence of the disappearance of 3-carboxyproxyl provides a parameter directly related to the concentration of $\cdot\text{OH}$. It is also expected that the validity of the technique could be tested by comparing results to those achieved by the traditional spin-trapping methods recently reported.¹² To provide further mechanistic information a quantitative analysis of the products produced by photolysis of aqueous solutions of 3-carboxyproxyl in the presence of TiO_2 was undertaken. The quantum yield for formation of $\cdot\text{OH}$ and the photon flux dependence of the rate of formation of $\cdot\text{OH}$ are all found to be consistent with recently published results confirming the quantitative validity of the 3-carboxyproxyl spin trap method.

Experimental Section

3-Carboxy-2,2,5,5-tetramethyl-1-pyrroldinyloxy (3-carboxyproxyl) and its sodium salts were purchased from Aldrich and used without further purification. 2,2,5,5-Tetramethyl-3-pyrrolidine-3-carboxamide was also purchased from Aldrich and hydrolyzed to 3-carboxy-2,2,5,5-tetramethylpyrrolidine (proxyl-NH). The samples containing 0.20 g L^{-1} Degussa P-25 TiO_2 and $8.0 \times 10^{-4} \text{ mol L}^{-1}$ 3-carboxyproxyl, unless otherwise noted, were prepared in deionized water (Millipore water

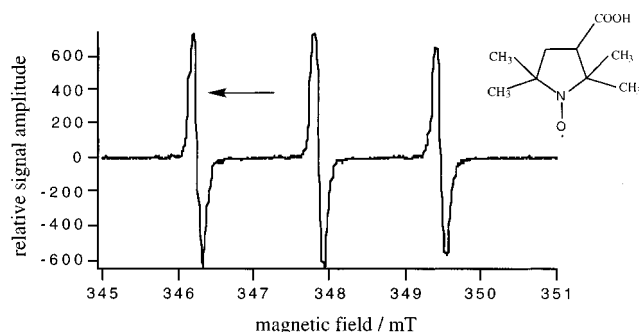


Figure 1. EPR signal and structure of 3-carboxyproxyl in an aqueous solution (pH = 3.8). EPR spectrometer settings: center field, 348 mT; sweep width; 6 mT; number of scans, 10. Microwave frequency: 9.78 GHz. The arrow indicates the peak used for height measuring.

purification system) and sonicated for 10 min. The pH values for the flash photolysis experiments were adjusted with HClO_4 and NaOH .

EPR Experiments. The EPR spectra were recorded using a Bruker ESP 380 ESR spectrometer, operating at the X band. Data acquisition and instrument control were achieved by using Bruker's ESP 380 E software. The samples were examined in a fused silica cell inside a rectangular TE_{102} (Bruker ER 4102ST) cavity of the EPR instrument. In order to record the consumption of 3-carboxyproxyl in the irradiated solutions, the height of the low-field EPR line (Figure 1) was monitored as a function of time.

O_2 Concentration. To control the concentration of molecular oxygen, the samples were bubbled with air for 15 min, prior to the EPR experiments. To examine the influence of the oxygen concentration on the 3-carboxyproxyl consumption, the samples were bubbled with a mixture of prepurified O_2 and N_2 for 40 min before the experiments. During the equilibration process, the samples were isolated from surrounding air by rubber stoppers.

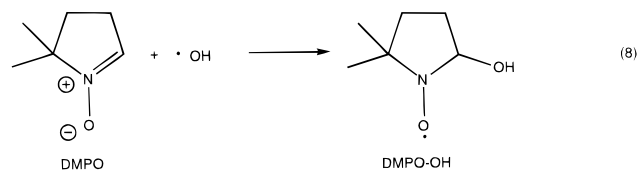
Photon Flux. The samples inside the optical cavity of the EPR instrument were illuminated by a Xe lamp (LX300 UV) whose output passed through a H_2O infrared filter of 10 cm path length with a UV filter WG 280 (CVI Laser Cooperation) inside and then focused onto the cell with a quartz lens. To examine the influence of the light intensity on the 3-carboxyproxyl consumption, neutral density filters were placed between the lamp and the IR cell. For the flash photolysis experiments, a frequency-tripled Nd-YAG laser ($\lambda_{\text{ex}} = 355 \text{ nm}$ with flash duration, ca. 15 ns) was used. The TiO_2 loading for these experiments was 0.002 g L^{-1} .

Photolysis. The photolysis experiments were carried out using a TQ 150 (Heraeus) lamp illuminating an aqueous, unbuffered, air-saturated 400 mL solution of 0.20 g L^{-1} Degussa P-25 TiO_2 and $8.0 \times 10^{-4} \text{ mol L}^{-1}$ 3-carboxyproxyl. The spectral emittance of the lamp between 200 and 400 nm was determined by uranyl oxalate actinometry to be 11 W. The solution samples (5 mL) were taken at approximately 0, 60, 120, 180, 240, 300, 360, 420, 480, 540, and 600 s and filtered through $0.22 \mu\text{m}$ nylon-syringe-filter (Roth). The TiO_2 residue was then washed with 5 mL CHCl_3 . The solution of 3-carboxyproxyl and the reaction products were injected into a gas chromatograph (GC) (HP 5971A MSD (mass selective detector), coupled with a HP 5965B ID (infrared detector)). The injection volume was 0.10 mL. An HP-INNOWAX capillary column (cross-linked polyethylene glycol) was employed. All reaction products were identified by IR and mass spectroscopy (MS). For the structural determination of the reaction products formed, authentic samples of 3-carboxyproxyl and proxyl-NH were employed as standards. The same GC/MS response factor of

3-carboxyproxyl and 2,2,5,5-tetramethyl-3-carboxypyrollidine oxime (proxyl-OH) was assumed for quantitative determination of products. For the dimer, it was estimated that the GC/MS response is 2 times that of 3-carboxyproxyl.

Results and Discussion

The Spin-Trapping Method for Determining the Generation of •OH. The EPR spin-trapping technique, developed by Janzen and Blackburn,¹⁴ was adapted by Jaegar and Bard to trap •OH produced in the irradiation of aqueous solutions of TiO₂. The basic concept of an EPR spin trap is that a diamagnetic radical scavenger (e.g., DMPO)¹⁰ serves as an efficient scavenger of reactive free radicals to produce an EPR signal of the nitroxide adduct that results from addition. In favorable cases the structure of the trapped radical can be inferred from the hyperfine coupling observed in the nitroxide adduct. For example, the addition of •OH to DMPO (eq 8)



occurs with a rate constant close to that of a diffusion-controlled reaction (ca. $3\text{--}4 \times 10^9 \text{ M}^{-1} \text{ s}^{-1}$) to form a nitroxide (DMPO-OH) with a characteristic EPR splitting pattern. Sun has determined the fraction of DMPO-OH among all the products to be ca. 33%, a quantity termed the “trapping efficiency”, η .¹⁹ The trapping efficiency is a chemical yield based on the spin trap converted to product. The efficiency η should not be confused with the quantum efficiency Φ , which is based on the number of photons absorbed, a difficult quantity to measure in a highly scattering medium. Colussi et al.¹³ employed DMPO to determine the quantum yield for photogenerated hydroxyl radicals in irradiated TiO₂ solutions to be $\Phi = 0.04$. This value was in good agreement to that determined by Sun and Bolton,¹⁹ employing a quantitative analysis of the products derived from the attack of •OH on methanol.

In many respects, the spin-trapping method employing 3-carboxyproxyl (eq 3) in this report to track the production of •OH is directly analogous to the conventional method employing DMPO (eq 8). The main difference is a technical one in that the *disappearance* of an EPR signal is monitored rather than the *appearance* of an EPR signal. The technique reported here has an advantage in simplicity, but suffers from the lack of direct information on the chemical fate of the spin trap. It was therefore of prime importance to quantitatively determine the products derived from reaction of 3-carboxyproxyl and to correlate the results with those reported for DMPO.

EPR of 3-Carboxyproxyl in Aqueous Solutions Containing TiO₂. The EPR spectrum of aqueous solutions of 3-carboxyproxyl show the well-known three-line spectrum of a nitroxide (Figure 1) resulting from ¹⁴N hyperfine coupling ($a^N = 1.6045 \text{ mT}$). Two standard parameters are readily derived from the EPR spectra of nitroxides: the average polarity of the microscopic environment of the spin probe derived from the analysis of the coupling constants, and the rotational mobility of the spin probe derived from the simulation of the spectrum and computation of the rotational correlation time, τ_c , of the spin probe. Both parameters have the potential to report interactions of the spin trap with the TiO₂ surface. The correlation times, τ_c , for motion of 3-carboxyproxyl were evaluated from the observed EPR spectra by means of the simulation program of Schneider and Freed.²⁰ Assuming that the spectra are charac-

teristic of the fast motion conditions ($\tau_c < 2\text{--}3 \times 10^{-9} \text{ s}$), the three nitrogen hyperfine lines of the spin trap 3-carboxyproxyl are modified in their relative widths for variations of the environmental microviscosity.²¹ In this case it is possible to calculate the widths of each hyperfine component by the simplified formula^{22,23}

$$\Delta H(m_N) = A + Bm_N + Cm_N^2 \quad (9)$$

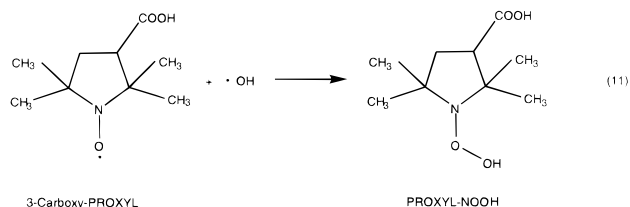
In this formula A represents both contributions from the anisotropies of the g tensor (Zeeman coupling) and the A_N tensor (hyperfine coupling) and terms which are not motionally based. The remaining B and C terms also contain the anisotropic components of the g and A tensors and the spin densities in terms of two correlation times for motion, τ_B and τ_C , respectively. With the known line widths of the three m_N manifolds and assuming an anisotropic Brownian motion where $\tau_B \neq \tau_C$, the values of τ_B and τ_C can be calculated by the simplified formulas

$$\tau_B = B^* \Delta H_0 [(h_0/h_1)^{1/2} - (h_0/h_{-1})^{1/2}] \quad (10a)$$

$$\tau_C = C^* \Delta H_0 [(h_0/h_1)^{1/2} + (h_0/h_{-1})^{1/2} - 2] \quad (10b)$$

In the above equations, h_i represents the peak heights. Using the value $B^* \approx C^* \approx 6.5 \times 10^{-10}$ for nitroxide radicals in water solution^{24–26} and $\tau_c = (\tau_B \tau_C)^{1/2}$, we have calculated the correlation time, τ_c , for motion of 3-carboxyproxyl in water at pH = 3.7 to be 38 ps. Addition of 2.3 g L⁻¹ to the sample causes an increase of the value of τ_c to 45 ps. Though the effect is not large, the increased values of τ_c are indicative of an interaction of the spin probe with the TiO₂ surface.

Irradiation of Aqueous Solutions of 3-Carboxyproxyl Containing TiO₂. Irradiation (280 nm < λ < 400 nm) of an aqueous solution of 3-carboxyproxyl (0.8 mM) in the presence of TiO₂ (0.2 g L⁻¹) results in a decrease of the EPR signal but not in a measurable change in the shape of the signal. A straightforward adaptation of the conventional scheme for the mechanism of steady-state photomineralization of organic molecules by TiO₂ is given in Scheme 1 in which an elementary reaction step and a corresponding rate expression are given. Asmus, employing the pulse radiolysis technique, measured the rate of addition of •OH radicals to 3-carboxyproxyl derivatives to be close to that of diffusion-controlled reactions (ca. $3.7 \times 10^9 \text{ M}^{-1} \text{ s}^{-1}$), an expected value from literature values of reactive radicals to nitroxides.^{27–29a} The structure of the primary product of addition was postulated to be the adduct proxyl-NOOH (eq 11). However, no product analyses were reported.



Ollis et al. found that in the case of hydroxyl radicals the average distance of molecular diffusion depends on the concentration of the substrate [S] and the rate constant for the reaction between •OH radicals and the substrate.^{29b} Using [S] = 10⁻³ M and a second-order rate constant on the order of 10⁹ M⁻¹ s⁻¹, the characteristic diffusion length is around 10⁻⁸ m.^{29b} On the basis of these findings, we would expect hydroxyl radicals not to diffuse very far into the solution, but to react directly or at least considerably close to the surface. In the

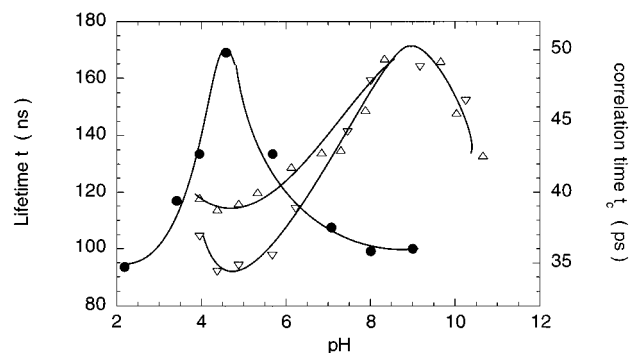


Figure 2. Lifetime of the conducting band electrons with (Δ) and without (∇) 3-carboxyproxyl (0.8 M). $[\text{TiO}_2] = 0.015 \text{ g L}^{-1}$. Plot also indicates the correlation time τ_c (\bullet) for the spin trap at different pH values. The lifetimes were determined from the kinetic absorption traces recorded at $\lambda_{\text{abs}} = 620 \text{ nm}$ ($\lambda_{\text{exc}} = 355 \text{ nm}$, 22 °C). EPR spectrometer settings: center field, 348 mT; sweep width, 6 mT; number of scans, 5. Microwave frequency: 9.78 GHz.

case of surface-bound substrates the characteristic diffusion length should even be smaller due to the closer distance to the reaction sites. We have determined the binding constant for 3-carboxyproxyl ($8 \times 10^{-5} \text{ M}$ up to $8 \times 10^{-3} \text{ M}$) on TiO_2 (0.2 g L^{-1}) in an aqueous solution at $\text{pH} = 3.8$ to be $1.4 \times 10^4 \text{ M}^{-1}$, using the Langmuir model of adsorption. At a 3-carboxyproxyl concentration of 0.8 mM, 95% of all spin trap molecules are adsorbed on the TiO_2 surface, and therefore we expect eq 11 to take place with hydroxyl radicals either still bound to the particle surface or very close to it. Further work detailing the influence of the pH on the trapping process will be reported elsewhere.

Although the disappearance of the signal of 3-carboxyproxyl can be reasonably attributed to eq 11, it is also plausible that the disappearance could be due to reaction with conduction band electrons or species derived from these electrons, e.g., $\bullet\text{O}_2^-$. Indeed, the reaction of nitroxyl derivatives related to 3-carboxyproxyl are reported²⁸ to react with hydrated electrons with rate constants of the order of $10^{10} \text{ M}^{-1} \text{ s}^{-1}$. As a result, we investigated the reaction of our spin trap with conduction band electrons of TiO_2 produced by photoexcitation.

Conducting band electrons give a pH-sensitive absorption spectrum revealing a broad absorbance with a maximum around 800 nm under alkaline conditions.² Lowering the pH shifts the spectrum to the blue, showing a new maximum around 600 nm. Taking advantage of the characteristic absorption band, we have recorded the temporal evolution of the transient spectrum ($\lambda_{\text{abs}} = 620 \text{ nm}$) at different pH values after excitation of the semiconductor particles with a frequency-tripled (355 nm) ND laser pulse.

The lifetime τ of the conduction band electrons in the presence and absence of 3-carboxyproxyl as a function of pH is shown in Figure 2 (left ordinate). There is no significant change in lifetime in the pH range 7–11 and a maximum change in lifetime (from ca. 120 ns to ca. 90 ns) around pH 4.8. The value of τ_c for 3-carboxyproxyl was determined (Figure 2, right ordinate) in the same pH range, and a maximum value of τ_c was found at $\text{pH} = 4.8$, i.e., the same pH for which the conduction band electrons undergo maximum quenching by 3-carboxyproxyl. These results suggest that there is a certain amount of reaction of 3-carboxyproxyl with conduction band electrons. The increased value of τ_c indicates an increased interaction of the spin trap at $\text{pH} = 4.8$, consistent with a more efficient reaction with the conduction band electrons that have made their way to the TiO_2 surface. These findings also reflect the electrostatic interactions between the spin trap and the

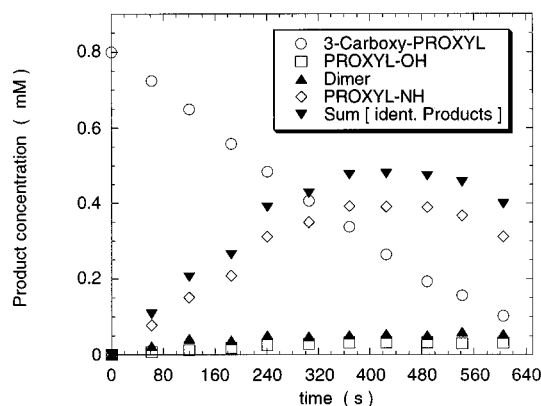
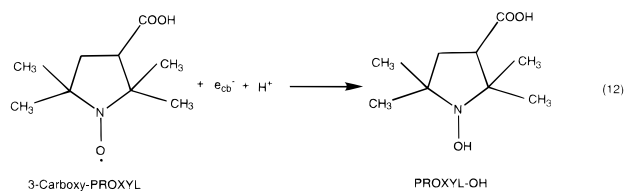


Figure 3. Photolysis of 3-carboxyproxyl (0.8 mM) in the presence of TiO_2 (0.2 g L^{-1}). For experimental details see Photolysis part in Experimental Section.

semiconductor surface. In the pH range 4–6 the probe molecules are strongly attached to the surface due to the deprotonated carboxyl group ($\text{p}K_{\text{A}} \approx 3.9$) and the positively charged TiO_2 surface (isoelectric point of Degussa P25 $\text{TiO}_2 = 6.1^{29c}$). For $\text{pH} = 3.8$ we found a binding constant of $1.4 \times 10^4 \text{ M}^{-1}$. When the pH is increased above 6, the surface charge becomes negative and the negatively charged spin probe is repelled from the surface, which is displayed by a decrease of the correlation time τ_c . Lowering the pH below 4 results in the protonation of the carboxyl group and therefore in a weaker interaction between adsorbent and adsorbate which also leads to lower values for τ_c . The reduction of nitroxides with electrons is expected to produce reduction products such as proxyl-OH (eq 12).

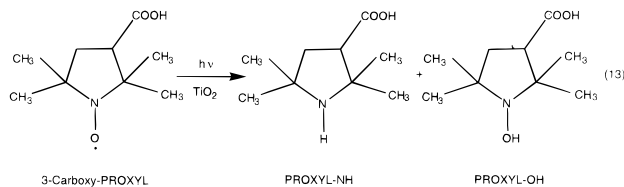


Product Analysis. Product analyses are of considerable importance in any mechanistic analysis. In the case of products formed from strongly oxidizing and strongly reducing conditions as those present when TiO_2 is photoexcited, primary products may rapidly be converted to secondary products, so there is no guarantee that isolated products are primary unless conversions are kept low and proper controls are conducted.

Aqueous solutions of 3-carboxyproxyl kept in the dark are stable for weeks. With added TiO_2 (0.2 g L^{-1}) no observable change in the 3-carboxyproxyl could be observed in the dark within 2 weeks. The illumination ($200 \text{ nm} < \lambda < 400 \text{ nm}$) of a TiO_2 -free solution of 3-carboxyproxyl produces a decrease of the spin trap concentration from the initial $8 \times 10^{-4} \text{ M}$ to $7.2 \times 10^{-4} \text{ M}$ within 10 min due to the reactions of photoexcited nitroxides with themselves.^{30a}

A quantitative analysis was made of the products produced by the steady-state photolysis ($200 \text{ nm} < \lambda < 400 \text{ nm}$) of aqueous solutions of 3-carboxyproxyl (0.8 mM) in the presence of TiO_2 (0.2 g L^{-1}) at $\text{pH} = 3.8$. Aliquots of samples were taken from the photolysis medium at minute intervals and subjected to GS, MS, and IR analysis. The results are summarized in Figure 3. Three experiments were run per point and the maximum deviation was 7% of the reported value. Two products, proxyl-NH and proxyl-OH, were identified unambiguously by comparison of the GC retention time, MS cracking pattern, and IR spectrum to authentic materials.

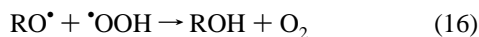
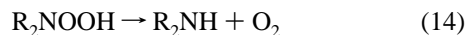
Under the conditions employed for photolysis, the initial concentration of 3-carboxylproxyl decreased from 0.8 to 0.11 mM within 10 min. At the lowest conversions the disappearance of 3-carboxylproxyl is accompanied by the appearance of a single major product, proxyl-NH (eq 13), and a minor product,



proxyl-OH. A second minor product corresponding to a "dimer" of 3-carboxylproxyl (vide infra for proposed structure) was detected by MS ($m/e = 370.44$ mu).

To examine the possibility of a direct oxidation of the spin trap by photogenerated holes, we carried out the photolysis in an acetonitrile/methanol (1:1) mixture, where hydroxyl radicals are not expected to have a major impact on the reaction. An air-saturated suspension containing 0.8 mM 3-carboxylproxyl and TiO₂ (0.2 g L⁻¹) was illuminated (200 nm < λ < 400 nm) for 10 min. Under these conditions the initial concentration of the spin trap decreases from 0.8 to 0.68 mM. Besides traces of unidentified products only one major product appears, which could be identified as proxyl-OH. While the generation of proxyl-OH can be attributed to either a reduction process with conducting band electrons (eq 12) or the reaction of photoexcited spin traps with themselves,^{30a} the absence of any major oxidation product clearly indicates that hole trapping by the spin probe does not effectively compete with direct oxidation of the solvent. Carrying out the same experiment under a nitrogen atmosphere, we found almost the same results with slightly higher amounts of proxyl-OH produced.

Up to this point we have assumed that •OH is the reactive species involved in reaction with 3-carboxylproxyl, yet the structure of the major product, proxyl-NH, appears to indicate that a *reduction* has occurred. This apparent discrepancy may be rationalized by consideration of the most likely first step in the reaction of •OH with 3-carboxylproxyl to produce proxyl-NOOH as a primary product (eq 11) and proxyl-NH as a plausible secondary reaction of this primary product (eq 14). The unit R₂NOOH which is present in proxyl-NOOH is reminiscent of the ROOOH unit present in trioxides.^{30b} The later species undergo facile cleavage (eq 15), even at low temperatures. The formal disproportionation shown in eq 16 is a plausible pathway for reaction of the species produced in eq 15.

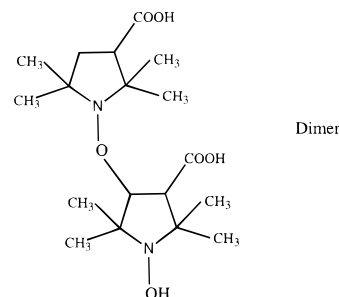


We propose that for proxyl-NOOH, the reactions analogous to eqs 15 and 16 could be possible. Notice that proxyl-NH is the product expected from disproportionation of a R₂N••OOH radical pair (eq 14). Recent calculations by Sumathi et al. have supported the possibility of the cleavage of unsubstituted H₂NOOH into NH₃ and O₂.^{30c} However, at this point the mechanism of product formation must be considered as speculative.

The appearance of proxyl-OH in the reaction process can be attributed to the reduction of 3-carboxylproxyl molecules by conducting band electrons and the subsequent addition of a

proton (eq 9). In this way proxyl-OH represents the reduced nitroxide species produced in the reaction leading to the different lifetimes of the conducting band electrons with and without the spin trap (Figure 2). The reductive pathway to proxyl-OH was also confirmed by running the same photolysis experiment under a nitrogen atmosphere. In the absence of any traces of oxygen, the quantity of generated proxyl-OH is remarkably higher as the result of the removal of an important path (eq 4) that competes with 3-carboxylproxyl for conducting band electrons.

We also consider the possibility that the illumination with wavelengths $\lambda < 200$ nm excites both the $\pi \rightarrow \pi^*$ and the $n \rightarrow \pi^*$ transitions of the N-O bond.^{30a} Nitroxides in the photoexcited state are much better hydrogen atom abstractors than in the ground state. Therefore, it is possible, that a certain part of proxyl-OH molecules have been formed via hydrogen abstraction from 3-carboxylproxyl or other species with abstractable hydrogens. A reaction involving hydrogen abstraction also explains the appearance of the third isolated product, with a mass peak = 370.44 mu corresponding to a "dimer" of 3-carboxylproxyl. From the mass spectrum and the IR absorption bands we propose that this product is a dimer based on two 3-carboxylproxyl molecules and coupled via the C₄ position of the first molecule and the N-O bond of the second molecule.



This observed dimer could arise from the reaction of a biradical formed via hydrogen abstraction with a second 3-carboxylproxyl molecule, similar to the addition of carbon-centered radicals to nitroxides. Corresponding reaction products, with the exception of proxyl-NH, were found by Keana from the photolysis of 4-hydroxy-2,2,6,6-tetramethylpiperidine-1-oxyl in toluene in the absence of a semiconductor.^{30a} The traces of unidentified products could be attributed to a photodecomposition of the spin trap, eliminating nitrogen oxide and leading to an olefin derivative.³¹

From the data of Figure 3 the trapping efficiency or chemical yield of proxyl-NH at low conversion can be computed. During the first 5 min of photolysis, the mass balance of the three identified products, proxyl-NH, proxyl-OH, and the dimer, almost exactly corresponds to the amount of 3-carboxylproxyl consumed, indicating that the amount of unidentified products is negligible. In this way we have calculated the trapping efficiency η for each time from eq 17.

$$\eta = [\text{proxyl-NH}] / ([\text{proxyl-NH}] + [\text{proxyl-OH}] + [\text{dimer}]) \quad (17)$$

The values derived from eq 17 for the trapping efficiency η of 3-carboxylproxyl with hydroxyl radicals vary between 0.82 and 0.78 giving an average trapping efficiency $\eta = 0.79$. This value may be compared to $\eta = 33\%$ reported for DMPO.¹² In this way it is possible to calculate the concentration of proxyl-NH at any given time by measuring the signal intensity of the spin trap 3-carboxylproxyl at that time. The difference between the corresponding concentration and the initial concentration of 3-carboxylproxyl multiplied by the trapping efficiency ($\eta =$

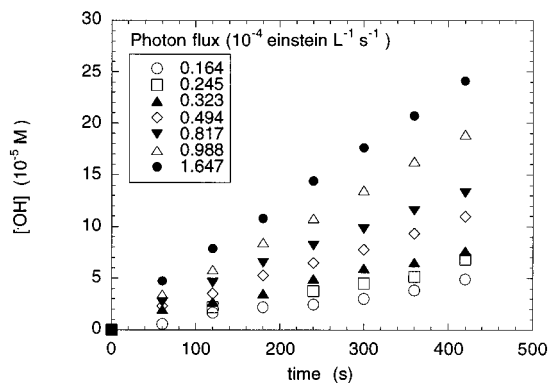


Figure 4. Hydroxyl radical concentration vs time at different light intensities, employing the EPR signals obtained by steady-state illumination ($280 \text{ nm} < \lambda < 400 \text{ nm}$) of a suspension containing 3-carboxyproxyl (0.8 mM) and TiO_2 (0.2 g L^{-1}).

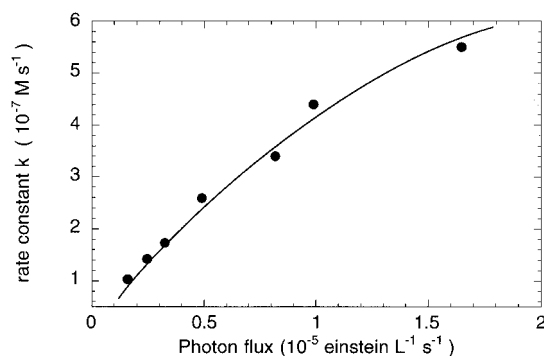


Figure 5. Dependence of the rate constant k (10^{-7} M s^{-1}) of the formation of hydroxyl radicals on the photon flux. The data are from Figure 4.

0.79) is the concentration of proxyl-NH. In the absence of other oxidizable compounds, the concentration of hydroxyl radicals directly corresponds to the proxyl-NH concentration (eq 3) and therefore has the same value.

Effect of Photon Flux on the Rate of Formation of $\cdot\text{OH}$.

During recent years, several contradicting results dealing with the dependence of photocatalytic rates on the photon flux I_0 were reported.^{33–35} Okamoto found a square root dependence,³⁶ but recent results favor, at least at lower light intensities, a linear correlation between the photon flux and the quantum yields for the production of hydroxyl radicals in illuminated TiO_2 suspensions.¹³ Applying 3-carboxyproxyl (0.8 mM) as the spin trap and using the derived trapping efficiency $\eta = 0.79$, we have calculated the production of $\cdot\text{OH}$ radicals at different light intensities (Figure 4) for an air-saturated suspension with TiO_2 (0.2 g L^{-1}) at $\text{pH} = 3.8$. The photon flux was in the range $1.64 < I_0 (\times 10^{-5} \text{ einstein s}^{-1}) < 16.4$. The illumination time chosen was 6 min, wherein the conversion of 3-carboxyproxyl to proxyl-NH, and thus the detectable generation of hydroxyl radicals, is almost linear. Figure 4 indicates that the criteria of a linear slope is reasonably fulfilled. With higher light intensities, the generation of hydroxyl radicals is increased. From the slopes in Figure 4, we have calculated the rate constant k (M s^{-1}) for the production of $\cdot\text{OH}$ radicals at different illumination strengths. Despite the fact that at longer time scales the production of proxyl-NH reaches a maximum and can be described with an exponential function, a linear fit to evaluate the rate constant k seems valid for the first few minutes. The result displayed in Figure 5 clearly shows that for low light intensities, the rate constants k for the hydroxyl production increase linearly with an increasing photon flux. Therefore, recent results supporting a linear dependence of the quantum

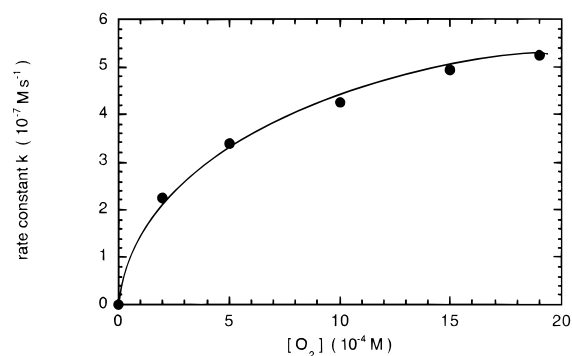


Figure 6. Effect of oxygen concentration on the rate constant k (10^{-7} M s^{-1}) of hydroxyl radical formation. Continuous irradiation ($280 \text{ nm} < \lambda < 400 \text{ nm}$) of a TiO_2 (0.2 g L^{-1}) suspension containing 3-carboxyproxyl (0.8 mM).

yield for the generation of DMPO-OH with an increasing light intensity are confirmed.¹³

Effect of Oxygen. Figure 6 shows the effect of the oxygen concentration on the rate constant of the hydroxyl generation. From degradation experiments with organic pollutants it is known that the mineralization efficiency with TiO_2 is dependent on the concentration of dissolved oxygen in the suspension.³² Oxygen acts as an electron acceptor, scavenging electrons from the conducting band (eq 4) and thus reducing the recombination rate (eq 7). The result in Figure 6 shows that an increasing amount of dissolved oxygen increases the rate constant of the $\cdot\text{OH}$ radical formation. The result is in good agreement with results derived by the DMPO method¹⁹ and by the mineralization of phenol in aqueous TiO_2 suspensions.³²

Effect of Added Sodium Salts. We have also examined the effect of dissolved sodium salts on the decrease of the spin trap signal and thus on the generation of proxyl-NH. An air-saturated suspension containing 3-carboxyproxyl (0.8 mM), TiO_2 (0.2 g L^{-1}), and different sodium salts ($[\text{NaX}] = 0.005\text{--}0.1 \text{ M}$) at $\text{pH} = 3.8$ was illuminated ($280 \text{ nm} < \lambda < 400 \text{ nm}$) for 7 min and the decrease in the signal intensity measured by EPR. From electrochemical potentials, sodium ions are not expected to interfere with the reduction process or the oxidation reactions by holes or hydroxyl radicals. Therefore upon addition of sodium salts, changes in the rate constant k for the production of proxyl-NH should be due to the influence of the corresponding anions. For the generation of DMPO-OH from DMPO , it was found that oxidizable compounds have a strong impact leading to lower rate constants.³⁷ Kochany has shown that the competition of various chlorophenols with DMPO toward $\cdot\text{OH}$ radicals in H_2O_2 solution obeys a linear Stern-Volmer relationship.³⁸ However, recent results derived by Colussi with DMPO in aqueous TiO_2 suspensions display a nonlinear effect of dichlorobenzene toward the generation of DMPO-OH .¹³

To investigate the effect of different sodium salts, 3-carboxyproxyl was used as a spin trap for hydroxyl radicals. Within the first 5 min of each illumination, the EPR signal of 3-carboxyproxyl decreased linearly, allowing linear fits from which the rate constant R for the generation of proxyl-NH can be derived. According to Kochany³⁸ and modified to our system, the rate R of the formation of proxyl-NH can be expressed as follows by eq 18.

$$R = d[\text{proxyl-NH}]/dt = k_3[3\text{-carboxyproxyl}][\cdot\text{OH}] \quad (18)$$

According to Scheme 1, the concentration of $[\cdot\text{OH}]$ is

$$[\cdot\text{OH}] = (I + k_4[\text{h}^+]) / (k_3[\text{3-carboxyproxyl}] + k_{6a}[\text{substrates}]) \quad (19)$$

Neglecting eq 7, it follows that

$$R = k_3[\text{3-carboxyproxyl}](I + k_4[\text{h}^+]) / (k_3[\text{3-carboxyproxyl}] + k_{6a}[\text{substrates}]) \quad (20)$$

R^0 is the rate of proxyl-NH formation when the concentration of the salts ([substrates]) = 0 and can be expressed as

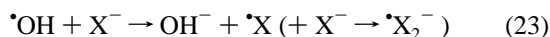
$$R^0 = (I + k_4[\text{h}^+]) \quad (21)$$

By solving eqs 20 and 21 with the initial concentrations [S]₀ and [3-carboxyproxyl]₀, eq 22 is obtained.

$$R_0^0/R_0 = 1 + k_{6a}[\text{substrates}]_0 / k_3[\text{3-carboxyproxyl}]_0 \quad (22)$$

The slopes of the plot R_0^0/R_0 vs [S]₀ give a value of $k_{6a}/k_3[\text{3-carboxyproxyl}]_0$ with an intercept of 1 (see Figure 7). The competition of the anions with 3-carboxyproxyl for hydroxyl radicals obeys a linear Stern-Volmer kinetic relationship. From the slopes in Figure 7 we have also estimated the rate constants k_{8a} for the reaction of $\cdot\text{OH}$ radicals with the anions. Using the rate constant $k_3 = 3.7 \times 10^9 \text{ M}^{-1} \text{ s}^{-1}$ for the reaction of 3-carboxyproxyl with hydroxyl radicals (eq 3)²⁸ and an initial concentration [3-carboxyproxyl]₀ = 0.8 mM, we obtained the rate constants k_{8a} shown in Table 1.

The results in Table 1 show that the rate constants k_{6a} for the reaction between $\cdot\text{OH}$ radicals and the anions are close to those that are diffusion-controlled. Among the rate constants for the three halides, the rate constants k_{8a} for the reaction



correspond with the decreasing potential of the corresponding redox couple $\text{X}^-/\cdot\text{X}_2^-$ in the sequence $\cdot\text{Cl}_2^- > \cdot\text{Br}_2^- > \cdot\text{I}_2^-$. The results derived with our method are therefore in good agreement with results obtained by Henglein using pulsed laser techniques.³⁹ However it should be noted that the author has attributed the reaction to a direct oxidation of adsorbed halides by valence band holes at pH = 1. We can not completely exclude a direct oxidation of surface-adsorbed halides, but according to results derived by Grabner and Quint the quantum yield for halide oxidation by holes and the concentration of adsorbed halides decrease with increasing pH of the solution.⁴⁰ We have employed a pH = 3.8, where the reaction of holes with surface OH groups is thermodynamically favored over halide oxidation. Therefore, we assume that halide oxidation in our case can be attributed primarily to the reaction with hydroxyl radicals.

Conclusions

3-Carboxyproxyl may serve as an alternate spin-trapping compound to detect hydroxyl radicals in illuminated TiO₂ solutions by electron paramagnetic resonance (EPR). The products generated during a photolysis of a 3-carboxyproxyl-containing TiO₂ suspension were analyzed, and the main species found was proxyl-NH. For the given 3-carboxyproxyl concentration (0.8 mM), the trapping efficiency $\eta = 0.82$ remains almost constant during the first 5 min of the illumination and allows the estimation of hydroxyl radical concentration released by the semiconductor particles. We could also confirm recent results that at lower light intensities, the rate for the $\cdot\text{OH}$ radical production rises linearly with an increasing photon flux.

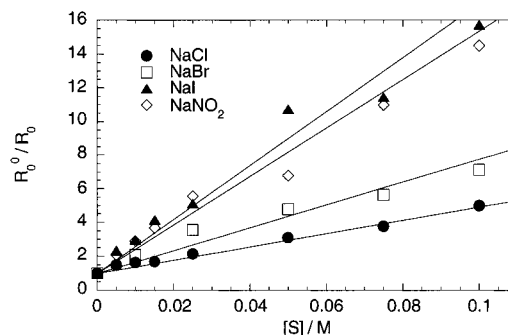


Figure 7. Inverse initial rate ratio R_0^0/R_0 (see text) vs salt concentration [S] for different salts.

TABLE 1: Rate Constants k_{6a} ($10^8 \text{ M}^{-1} \text{ s}^{-1}$) for the Reaction of $\cdot\text{OH}$ Radicals with Sodium Salts. Data Is Derived from Eq 22 and Figure 7

NaCl	NaBr	NaI	NaNO ₂
1.49	3.83	10.9	14.4

Furthermore, 3-carboxyproxyl as a spin trap was employed to examine the effect of oxygen as a scavenger for conducting band electrons. With an increasing concentration of dissolved O₂, the rate for the recombination between electrons and holes is diminished, and in this way, the generation of hydroxyl radicals slightly improved. In the presence of different sodium salts, the conversion of 3-carboxyproxyl to proxyl-NH is strongly affected by the anions, which compete with the spin trap for $\cdot\text{OH}$ radicals. The rate constants for the reaction between hydroxyl radicals and the anions, derived from the Stern-Volmer plots, are diffusion-controlled and dependent on the electrochemical potential of the redox couple.

Acknowledgment. The authors thank the National Science Foundation, NATO, Fond der Chemischen Industrie (foundation of the German Chemical Industry (VCI)), and BMBF for financial support of this work. P.F.S. thanks the Deutsche Forschungsgesellschaft (DFG) for a postdoctoral fellowship.

References and Notes

- (1) Fujishima, A.; Honda, K. *Bull. Chem. Soc. Jpn.* **1971**, *44*, 1148.
- (2) Graetzel, M. *Heterogeneous Photochemical Electron Transfer*; CRC Press, Inc.: Boca Raton, FL, 1989.
- (3) Fox, M. A.; Dulay, M. T. *Chem. Rev.* **1993**, *93*, 341.
- (4) Serpone, N. *Res. Chem. Intermed.* **1994**, *20*, 953.
- (5) *Photocatalytic Purification of Water and Air*; Ollis, D. F., Al-Ekabi, H., Eds.; Elsevier: Amsterdam, 1993.
- (6) *Photocatalysis: Fundamentals and Applications*; Serpone, N., Pelizzetti, E., Eds.; Wiley: New York, 1989.
- (7) Kraeutler, B.; Bard, A. J. *J. Am. Chem. Soc.* **1978**, *100*, 2239.
- (8) Frank, S. N.; Bard, A. J. *J. Phys. Chem.* **1977**, *81*, 1484.
- (9) Jaeger, C. D.; Bard, A. J. *J. Phys. Chem.* **1979**, *83*, 3146.
- (10) Harbour, J. R.; Chow, V. S. F.; Bolton, J. R. *Can. J. Chem.* **1974**, *52*, 3549.
- (11) Buxton, G. V.; Greenstock, C. L.; Helman, W. P.; Ross, A. B. *J. Phys. Chem. Ref. Data* **1988**, *17*, 717.
- (12) Riegel, G.; Bolton, J. R. *J. Phys. Chem.* **1995**, *99*, 4215.
- (13) Grella, M. A.; Coronel, M. E. J.; Colussi, A. J. *J. Phys. Chem.* **1996**, *100*, 16940.
- (14) Janzen, E. G. *Acc. Chem. Res.* **1971**, *4*, 31.
- (15) Moza, P. N.; Fytianos, K.; Samanidou, V.; Korte, F. *Bull. Environ. Contam. Toxicol.* **1988**, *41*, 678.
- (16) Neta, P.; Steenken, S.; Janzen, E. G.; Shetty, R. V. *J. Phys. Chem.* **1980**, *84*, 532.
- (17) Sun, L. Quantum Yield and Mechanism in TiO₂ Mediated Photocatalysis. Ph.D. Thesis, The University of Western Ontario, London, Ontario, Canada, 1994.
- (18) Carmichael, A. J.; Makino, K.; Riesz, P. *Radiat. Res.* **1984**, *100*, 222.
- (19) Sun, L.; Bolton, J. R. *J. Phys. Chem.* **1996**, *100* 4127.

- (20) Schneider, D. J.; Freed, J. H. In *Biological Magnetic Resonance. Spin Labeling. Theory and Applications*; Berliner, L. J., Reuben, J., Eds.; Plenum Press: New York, 1989; Vol. 8, p 1.
- (21) Ottaviani, M. F.; Cossu, E.; Turro, N. J.; Tomalia, D. A. *J. Am. Chem. Soc.* **1995**, *117*, 4387.
- (22) Kivelson, D. *J. Chem. Phys.* **1960**, *33*, 1094.
- (23) Jolicœur, C.; Friedman, H. L. *Ber. Bunsen-Ges. Phys. Chem.* **1971**, *75*, 248.
- (24) Martini, G.; Ottaviani, M. F.; Ristori, S.; Lenti, D.; Sanguineti, A. *Colloids Surf.* **1990**, *45*, 177.
- (25) Ristori, S.; Ottaviani, M. F.; Lenti, D.; Martini, G. *Langmuir* **1991**, *7*, 1958.
- (26) Ottaviani, M. F.; Ghatlia, N. D.; Turro, N. J. *J. Phys. Chem.* **1992**, *96*, 6075.
- (27) Gerischer, H. *Electrochim. Acta* **1993**, *38*, 3.
- (28) Nigam, S.; Asmus, K. D.; Willson, R. L. *Trans. Faraday Soc.* **1976**, *43*, 2324.
- (29) (a) Bowry, V. W.; Ingold, K. U. *J. Am. Chem. Soc.* **1992**, *114*, 4992. (b) Turchi, C. S.; Ollis, D. F. *J. Catal.* **1990**, *122*, 178. (c) Furlong, D. N.; Wells, D.; Sasse, W. H. F. *J. Phys. Chem.* **1986**, *90*, 1107.
- (30) (a) Keana, J. F. W.; Dinerstein, R. J.; Baitis, F. *J. Org. Chem.* **1971**, *36*, 209. (b) Nangia, P. S.; Benson, S. W. *J. Am. Chem. Soc.* **1980**, *102*, 3105. (c) Sumathi, R.; Engels, B.; Peyerimhoff, S. D. *J. Chem. Phys.* **1996**, *105*, 8117.
- (31) Keana, J. F. W.; Baitis, F. *Tetrahedron Lett.* **1968**, 365.
- (32) Okamoto, K.; Yamamoto, Y.; Tanaka, M.; Itaya, A. *Bull. Chem. Soc. Jpn.* **1985**, *58*, 2015.
- (33) Hoffmann, A. J.; Carraway, E. R.; Hoffmann, M. R. *Environ. Sci. Technol.* **1994**, *28*, 776.
- (34) Lepore, G. P.; Pant, B. C.; Langford, C. H. *Can. J. Chem.* **1993**, *71*, 2051.
- (35) Hong, A. P.; Bahnemann, D. W.; Hoffmann, M. R. *J. Phys. Chem.* **1987**, *91*, 2109.
- (36) Okamoto, K. *Bull. Chem. Soc. Jpn.* **1985**, *58*, 2023.
- (37) Savel'eva, O. S.; Shevchuk, L. G.; Vysotskaya, N. A. *J. Org. Chem. USSR (Engl. Transl.)* **1972**, *8*, 293.
- (38) Kochany, J.; Bolton, J. R. *J. Phys. Chem.* **1991**, *95*, 5116.
- (39) Henglein, A. *Ber. Bunsen-Ges. Phys. Chem.* **1982**, *86*, 241.
- (40) Grabner, G.; Quint, R. M. *Langmuir* **1991**, *7*, 1091.